International Journal of Pharmaceutics, 73 (1991) 163–169

ADONIS 0378517391002573

IJP 02453

Degradation of tragacanth by high shear and turbulent forces during microfluidization

Shawn Silvestri and Gustave Gabrielson

The University of Pittsburgh, Department of Pharmaceutical Sciences, 712 Salk Hall, Pittsburgh, PA 15261 (U.S.A.)

(Received 18 July 1990)
(Modified version received 1 March 1991)
(Accepted 20 March 1991)

Key words: Microfluidization; High shear degradation; Tragacanth; Capillary viscometry; Photon correlation spectroscopy

Summary

The mechanical degradation of tragacanth during exposure to microfluidization (Microfluidizer M110T, 23°C, modified high-pressure pump) was studied. Degradation was studied at inlet air pressures of 40, 60 and 80 psi which correspond to approximate pressures within the interaction chamber of 7500, 12500 and 17500 psi, respectively. It was observed that as exposure time to the turbulent and shear stress forces imposed by the Microfluidizer^{R} increased, intrinsic viscosity estimates decreased. Intrinsic viscosity decreases were correlated to apparent changes in the viscosity average molecular weight using the equivalent sphere model. Microfluidization-induced degradation was found to be first order in accordance with the Harrington Zimm modification of the random scission model for the mechanical degradation of polymers. At all three exposure pressures, tragacanth appeared to undergo shear degradation which required two distinct apparent degradation rate constants to describe the kinetic behavior. Plausible explanations are presented for the observed biphasic behavior.

Introduction

Polymers may be formulated into liquid-in-liquid dispersions as a therapeutic entity (e.g. proteins and peptides), as pharmaceutical adjuncts (e.g. interfacially active substances) or both. Previous research has shown that when high molecular weight compounds are subjected to harsh shearing forces in a viscous flow, the polymers may degrade (Morawetz, 1983). Moreover, a higher molecular weight compound is generally more sensitive to mechanical degradation than its corresponding lower molecular weight compound. Even the low shear force encountered in flow of a polymer through a conventional capillary viscometer may induce mechanical degradation if the number of passes through the capillary is sufficient (Moore and Parts, 1968).

During microfluidization of a liquid-in-liquid dispersion high shear, turbulent and cavitational forces simultaneously act on the dispersed phase to reduce droplet diameter (Korvstedt et al., 1984; Silvestri and Lostritto, 1989). Microfluidization has received great attention since it represents a novel approach to producing submicron emul-

---

Correspondence: S. Silvestri, The University of Pittsburgh, Dept of Pharmaceutical Sciences, 712 Salk Hall, Pittsburgh, PA 15261, U.S.A.

sions (mean droplet diameter under one micron) for pharmaceutical applications. In particular, submicron emulsions to increase drug solubility, lower injection volume, target drug delivery or control drug delivery have been addressed (Lostritto and Silvestri, 1987; Lostritto et al., 1987).

The objective of this research was to evaluate the effect(s) of microfluidization forces on the mechanical degradation of a model polymer. The combination of the high shear and turbulent forces encountered by a polymer in the interaction chamber of the Microfluidizer^{R} device may present sufficient energy to disrupt covalent bonds.

Harrington and Zimm did extensive work in theoretical and experimental aspects of shear-induced degradation of polymers and have reported that the process may be described as a first-order process if the shear stress to which the macromolecule is exposed exceeds a critical value (Harrington and Zimm, 1965) specific to the polymer.

In this study, gum tragacanth is chosen as a model surface-active macromolecule. Tragacanth has been used extensively in pharmaceutical preparations for its suspending, emulsifying, stabilizing, thickening, and adhesive properties which makes it an ideal candidate for evaluation of mechanical stability to microfluidization. In addition, the average molecular weight of tragacanth is approx. 840000 g mol^{-1} which is sufficiently large that changes in viscosity imparted by changes in average molecular weight may be readily detected by conventional rheological techniques such as capillary viscometry.

Theory

The intrinsic viscosity of a polymer is defined as:

$$\lim_{C\to 0} \ln(n_{\mathrm{rel}})/C = [n] \tag{1}$$

where n_{rel} is relative viscosity, C (g/cm^3) is the concentration of the polymer solute in solution and $[n]$ is the intrinsic viscosity (cm^3/g) of the polymer solute (Sperling, 1986). Intrinsic viscosity is a function of the average molecular weight of a polymer:

$$[n] = 2.5\frac{4\pi}{3}N\left(\frac{R_{e\theta}^2}{M}\right)^{3/2} M^{1/2}a^3 \tag{2}$$

where N is Avogadro's number, $R_{e\theta}$ is the radius of the hydrodynamically equivalent sphere in a theta solvent, M is the average molecular weight (g/mol) and a is the expansion coefficient for the polymer coil which accounts for expansion in a good solvent over that in a theta solvent (Flory, 1953). From Eqns 1 and 2 a direct link between relative viscosity and viscosity average molecular weight of the polymer exists through intrinsic viscosity.

Eqn 1 may be simplified. In the case of a dilute solution it is valid to approximate the intrinsic viscosity by:

$$\ln(n_{\mathrm{rel}})/C = [n]. \tag{3}$$

This equality is an approximation which is applicable only to infinitely dilute solutions. However, it should be noted that for any polymer solution concentration, the ratio on the left-hand side of Eqn 3 represents trends in intrinsic viscosity (or alternatively viscosity average molecular weight). It is convenient to consider relative viscosity in terms of the solution and pure solvent viscosities:

$$(n/n_0) = n_{\mathrm{rel}} \tag{4}$$

where n is the viscosity of the polymer solution at a specified concentration and n_0 is the viscosity of pure solvent (Flory, 1953). Both n and n_0 have units of g cm^{-1} s^{-1}.

In addition, Eqn 2 may be simplified. First, the ratio of $R_{e\theta}^2/M$ is approximately constant (Sperling, 1986). Further, all other terms with the exception of M on the right-hand side of Eqn 2 are constant under a specified set of conditions (e.g. specific solvent and temperature). Thus, Eqn 2 may be rewritten as:

$$[n] = BM^{1/2}. \tag{5}$$

where B ($\mathrm{mol}^{1/2}\ \mathrm{cm}^3\ \mathrm{g}^{-3/2}$) is an apparent constant.

The chemical kinetic theory of the mechanical degradation of macromolecules has been described in detail elsewhere (Harrington and Zimm, 1965). Briefly, for a polymer which undergoes moderate to extensive mechanical degradation from high shear and turbulent forces, the rate law for chemical degradation as described by changes in average molecular weight may be written as:

$$M_1 \frac{\mathrm{d}(1/M)}{\mathrm{d}t} = K \tag{6}$$

assuming limiting degradation to molecular weight M_1, where t is time and K is a first-order rate constant (time^{-1}). Eqn 6 may be rearranged to yield:

$$\frac{\mathrm{d}(1/M)}{\mathrm{d}t} = (K/M_1) = k \tag{7}$$

where k is an apparent first-order rate constant with units of $\mathrm{mol\ g^{-1}\ time^{-1}}$.

In terms of microfluidization-induced mechanical degradation, it is more convenient to work in terms of cycles through the device or volume passes rather than time. With this in mind, the working equations (Eqns 3, 5 and 7) become:

$$\ln(n_{\mathrm{rel},i})/C = [n]_i \tag{8}$$

$$[n]_i = BM_i^{1/2} \tag{9}$$

and

$$\frac{\mathrm{d}(1/M)}{\mathrm{d}i} = k \tag{10}$$

where i represents a designated number of volume passes through the Microfluidizer^R device and is directly related to exposure time.

Materials and Methods

Gum tragacanth powder N.F. (Ammend, Irvington NJ, Lot F14723G12) was used as received. Fresh double-distilled water (Corning Megapure 1) was used throughout.

Polymer solutions were prepared by dissolving 0.500 g of tragacanth in double-distilled water (final concentration 0.002 g cm^{-3}). The mixture was magnetically stirred at low speeds and at room temperature for approx. 15 min to allow complete dissolution (and/or swell) of the tragacanth powder.

The tragacanth solution was volumetrically split into three separate equal portions. Each portion was passed through a thermostatted (23°C) M110T Microfluidizer^R device (Microfluidics^R, Newton, MA) with a modified high-pressure pump at an inlet air pressure of 40, 60 or 80 psi. At each inlet air pressure, a 15 ml sample was collected after 0, 1, 2, 3 or 4 passes through the device. Four volume cycles were chosen as the upper limit based on the efficiency of the Microfluidizer^R as a homogenizer.

In order to eliminate time-dependent conformational effects post microfluidization, all samples were allowed to stand for 24 h under ambient conditions such that an effective equilibrium conformation might be achieved. Then efflux time (23°C) of each sample was determined with a Cannon Fenske Capillary Viscometer^R (Fisher Scientific). Measurements of efflux time were repeated until three values within a 0.5 s range of each other were obtained. These three efflux times were used to obtain an average ($n = 3$) efflux time. Average efflux time was then converted to absolute viscosity for further data analysis.

At 60 psi inlet air the microfluidization procedure was repeated on a second solution of tragacanth. A 15 ml aliquot was collected after each cycle, allowed to stand 24 h (ambient conditions) and was analyzed with photon correlation spectroscopy. Photon correlation spectroscopy studies (dynamic laser light scattering) were performed on an upgraded Nicomp^R 270 particle size analyzer (Nicomp^R, Santa Barbara CA). Data was collected as the volume mean diffusivity (proportional to volume average molecular weight) vs number of cycles. Particle sizing conditions were 23°C, data counts > 100K and $\chi^2 < 2$.

Results and Discussion

The following parameters were used in this analysis. The viscosity and density of water (23°C) were assumed to be 0.933 cps and 0.998 g cm^{-3}, respectively (CRC, 1985). The initial average molecular weight of tragacanth was taken to be 840 000 g mol^{-1} and the density of tragacanth was assumed to be approximately equal to that of water (Merck, 1983).

Viscosity data was collected as relative efflux time. Table 1 shows the average efflux time determined for the tragacanth solutions microfluidized 0 to 4 passes at inlet air pressures of 40, 60 and 80 psi. The averaged estimates of efflux time were converted to estimates of absolute viscosity using the relationship:

$$n = n_0 t / t_0 \qquad (11)$$

where t is the average efflux time of the sample and t_0 is the efflux time of pure water (Van Wazer, 1963). The approximated values of absolute viscosity are given in Table 1.

TABLE 1

Efflux times, absolute viscosities, intrinsic viscosities and viscosity average molecular weight estimates for tragacanth solutions exposed to microfluidization forces

Cycle	t (s)	n (cps)	$[n]$ (cm^3/g)	M (g/mol)
40 psi inlet air pressure				
0	124.2	2.11	407	840000
1	116.7	1.98	376	716395
2	111.2	1.89	352	627356
3	97.3	1.65	285	411838
4	93.2	1.58	264	351987
60 psi inlet air pressure				
0	124.2	2.11	407	840000
1	112.8	1.91	359	653089
2	105.6	1.79	326	538598
3	84.1	1.43	212	228132
4	82.1	1.39	200	202985
80 psi inlet air pressure				
0	124.2	2.11	407	840000
1	103.9	1.76	318	512117
2	95.0	1.61	273	378001
3	74.3	1.26	150	114357
4	70.7	1.20	125	79671

Regardless of the inlet air pressure (40, 60 or 80 psi), the absolute viscosity of the tragacanth solution was observed to decrease on increasing exposure time to the forces of microfluidization. This suggests mechanical degradation of tragacanth on exposure to the high shear and turbulent forces encountered during microfluidization.

The inlet air pressure appears to play a role in the relative reduction of absolute viscosity. That is, absolute viscosity is reduced the most (43%) for samples microfluidized at 80 psi inlet air pressure. This is followed by 60 psi (34% reduction) and 40 psi (25% reduction) inlet air pressure, respectively.

As the inlet air pressure is increased, the amount of shearing and turbulent forces encountered in the interaction chamber also increases. Inlet air pressure is a reflection of the pressure inside the interaction chamber. However, it is not the interaction chamber pressure itself. A 23 000 psi Haenni pressure gauge inserted inline immediately prior to the interaction chamber revealed that the inlet air pressures used in these studies correspond to approximate pressures of 7500 (40 psi), 12 500 (60 psi) and 17 500 (80 psi) lb per inch^2 (on the downstroke) within the interaction chamber. This is direct evidence in support of the effect of microfluidization forces encountered in the interaction chamber on the mechanical stability of polymers.

From Eqn 8, the intrinsic viscosity may be approximated. Table 1 summarizes the estimated values of intrinsic viscosity. As expected, changes in intrinsic viscosity correspond linearly to the observed changes in absolute viscosity by virtue of the approximation used.

From Eqn 9, having estimated the intrinsic viscosity in the absence of microfluidization ($i = 0$) and knowing the initial average molecular weight for tragacanth, B was estimated to be 0.444 $\mathrm{mol}^{1/2}$ cm^3 $\mathrm{g}^{-3/2}$. The value of B is constant and is assumed to be independent of viscosity average molecular weight. Therefore, from Eqn 9 where $i = 1$, 2, 3 or 4 the experimental estimates of intrinsic viscosity under the various processing conditions may be used to estimate viscosity average molecular weight. These values are given in Table 1. Note that the estimates of viscosity average molecular weight consistently decrease with either increasing number of cycles at a constant inlet air pressure or increasing inlet air pressure at a constant number of cycles.

In accordance with the theoretical treatment proposed by Zimm and Harrington a plot of $1/M$ vs cycles should give an apparent first-order rate constant for high shear-induced degradation (Harrington and Zimm, 1965). Fig. 1 depicts the $1/M$ versus cycles behavior for the three inlet air pressures. Interestingly, in all three cases a bi-linear relationship is observed. Two linear portions with distinctly different slopes are observed and the break or change in slope in all cases occurs after the second pass. Two plausible explanations for this phenomenon include: A change in mechanical degradation mechanism may occur or the initial slope may represent an approach to random scission kinetics. In either case, two distinct rate constants are required to describe the time course over the experimental time range.

Table 2 lists the results of the linear regressions of $1/M$ vs cycles. In all cases, the correlation coefficient for the linear regressions are greater than 0.937. This agrees with the proposed bi-linear analysis. In all cases, the second linear phase (greater than 2 passes) has a greater apparent rate constant for high shear induced degradation. A possible explanation for this phenomenon is as follows. If the limiting molecular weight for a specific polymer is assumed to be a constant for the device and dependent solely on the inlet air pressure, then M_l must remain constant over the entire exposure time and thus the first-order rate constant must be changing. It may be that initial energies supplied by microfluidization are in part used to shear or tear open the long chains. After the polymer chains are opened they would become more susceptible to microfluidization induced degradation as a greater number of bonds are directly accessible to the mechanical stress pockets produced during microfluidization (Harrington and Zimm, 1965).

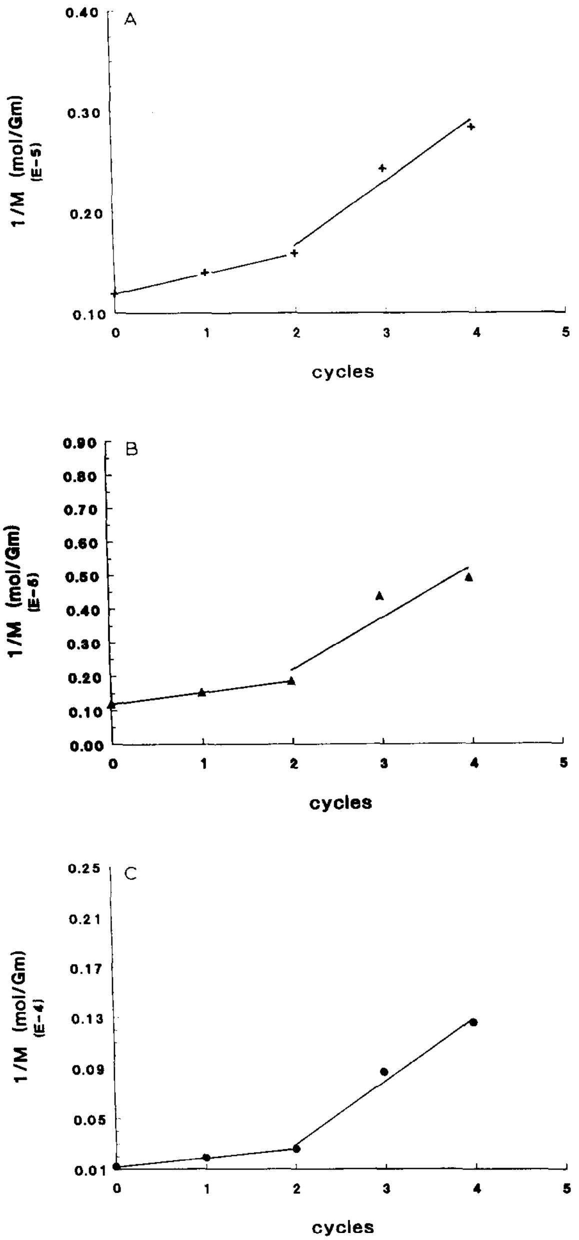

Fig. 1. Determination of apparent rate constants for the microfluidization induced degradation of tragacanth. Solid lines represent the linear regression for data over the range of the line. Processing conditions depicted are interaction chambers of 7500 (+), 12500 (▲) and 17500 (●) psi.

From the Zimm Harrington analyses, interaction chamber pressure would appear to have an effect on the apparent rate constant (k). Either M_l, K or both may be affected by changes in interaction chamber pressure. As interaction chamber pressure increases, the value of k is observed to increase. In other words, increased inlet air pressures lead to greater polymer sensi-

TABLE 2

Zimm-Harrington analyses for tragacanth mechanical degradation during microfluidization

Inlet air pressure (psi)	Cycle range	k (mol g^{-1} $cycle^{-1}$)	r
40	0–2	$2.02E-7$	0.9999
40	2–4	$6.24E-7$	0.9815
60	0–2	$3.33E-7$	0.9999
60	2–4	$1.53E-6$	0.9369
80	0–2	$7.28E-7$	0.9996
80	2–4	$4.95E-6$	0.9912

tivities to mechanical degradation. This may result from one of three mechanisms: M_l may decrease as interaction chamber pressure increases, K may increase as interaction chamber pressure increases, or a simultaneous decrease in M_l and increase in K may occur as interaction chamber pressure increases. The exact nature of the increase in tragacanth sensitivity on increasing interaction chamber pressures is presently under investigation.

To ensure that the primary factor contributing to decreases in viscosity was mechanical degradation and to validate the sensitivity of viscosity to molecular weight, photon correlation spectroscopy studies were conducted on samples subjected to 60 psi inlet air pressure. These results are listed in Table 3 as the volume mean diffusivity (D_v) vs number of passes. Tragacanth was found to possess a unimodal log volume distribution. The volume mean diffusivity may be related to volume mean molecular weight (M_v) through:

$$M_v = (S/D_v)^2 \tag{12}$$

for a random coil macromolecule (Kinsinger, 1975). Using the known initial average molecular weight (840 000 g mol^{-1}) and the experimental diffusivity ($1.41E-9$ cm^2 s^{-1}), S was approximated as $1.292E-6$ cm^2 s^{-1} $g^{1/2}$ $mol^{-1/2}$. This value of S was used to estimate M_v after each cycle (Table 3). Viscosity average molecular weights were slightly larger than volume average molecular weights. This is expected behavior (Sperling, 1986). Analysis of the $1/M_v$ vs time relationship gave bi-linear behavior with initial slope (0–1 cycle) $9.60E-7$ mol g^{-1} $cycle^{-1}$ and terminal slope (1–4 cycles) equal to $1.50E-6$ mol g^{-1} $cycle^{-1}$ ($r = 0.986$). These estimates are in agreement with the viscosity estimates given in Table 2. This study supports the case for mechanical degradation as the primary degradation process. Moreover, it validates the use of viscosity estimates of average molecular weight as a simple and inexpensive technique to study the mechanical degradation of tragacanth.

TABLE 3

Photon correlation spectroscopy studies for tragacanth microfluidized at 60 psi inlet air pressure

Cycle	D_v (cm^2 s^{-1})	M_v (g mol^{-1})
0	$1.41E-9$	840000
1	$3.22E-9$	161000
2	$3.46E-9$	139000
3	$3.97E-9$	106000
4	$4.18E-9$	95500

Summary

The effects of the forces associated with a novel homogenization process (microfluidization) on the mechanical stability of a model polymer (tragacanth) have been evaluated. Estimates of absolute viscosity of a dilute tragacanth solution were made using conventional capillary viscometry techniques. These techniques appear to be sensitive enough to detect changes in viscosity which arise on exposure of tragacanth solutions to microfluidization as evidenced by agreement with photon correlation spectroscopy studies.

The origin of the viscosity changes is thought to be related to changes in the average molecular weight of the polymer on exposure to high shear and turbulent forces. A modified form of the equivalent sphere model was used to correlate intrinsic viscosity estimates to viscosity average

molecular weight estimates. Subsequently, Zimm Harrington plots were constructed and apparent first-order degradation constants were estimated.

Tragacanth degradation on exposure to the high shear and turbulence of microfluidization appears to be substantial and dependent on exposure time as well as interaction chamber pressure. For longer exposure times, at a specified inlet air pressure, a greater decrease in the viscosity average molecular weight was observed. For higher interaction chamber pressure, at a specified exposure time, a greater decrease in the viscosity average molecular weight was observed.

Two distinct rate constants were required to describe degradation kinetics at each interaction chamber pressure studied. This suggested either a change in the mechanical degradation mechanism or an approach to random scission kinetics.

The observation that the microfluidization process may degrade polymer substances could have impact on the formulation of a disperse system. In general, it may be desirable to avoid subjecting a high molecular weight compound to microfluidization without first determining whether or not the compound is stable to the shear and turbulent forces it will encounter in the interaction chamber. If the polymer fragments produced on the exposure of a susceptible surface-active polymer to microfluidization possess the necessary interfacial activity and lack toxicity, stability to microfluidization may not be an issue. Certainly, degradation of a macromolecular therapeutic entity by microfluidization would preclude subjecting this type of a compound to this particular homogenization technique. In this case, the problem may be avoided by homogenization in the absence of the therapeutic entity and subsequently adding the drug to the microfluidized drug free dispersion.

Acknowledgements

This work was supported in part by the University of Pittsburgh, School of Pharmacy and the University of Pittsburgh Central Research Development Fund.

References

Becher, P., *Encyclopedia of Emulsion Technology*, Vol. 1, *Basic Theory*, Dekker, New York, 1985.

CRC Handbook of Chemistry and Physics, 66th Edn, CRC Press, Boca Raton, FL, 1985.

Flory, P., *Principles of Polymer Chemistry*, Cornell University Press, Ithaca, New York, 1953.

Harrington, R. and Zimm, B., Degradation of polymers by controlled hydrodynamic shear. *J. Phys. Chem.*, 69 (1965) 161–175.

Kinsinger, J., Macromolecules: Their masses, sizes and related distributions. In Burke, J. and Weiss, V. (Eds), *Characterization of Materials in Research: Ceramics and Polymers*, Syracuse University Press, Syracuse, NY, 1975.

Korvstedt, H., Bates, R., King, J. and Siciliano, A., Microfluidization. *D & CI*, November (1984) 36–40.

Lostritto, R., Goei, L. and Silvestri, S., Theoretical considerations of drug release from submicron oil in water emulsions. *J. Parent. Sci.*, 41 (1987) 214–219.

Lostritto, R. and Silvestri, S., Temperature and cosurfactant effects on lidocaine release from submicron oil in water emulsions. *J. Parent. Sci.*, 41 (1987) 220–224.

Merck Index, 10th Edn, Merck and Co., Rahway, NJ, 1963.

Moore, D. and Parts, A., Mechanical degradation of polystyrene in solution. *Polymer*, 9 (1968) 52–53.

Morawetz, H., *Macromolecules in Solution*, Krieyer, Malabar, FL, 1983.

Silvestri, S. and Lostritto, R., Theoretical evaluation of dispersed droplet radii in submicron oil in water emulsions. *Int. J. Pharm.*, 50 (1989) 141–146.

Sperling, L., *Physical Polymer Science*, Wiley, New York, 1986.

Van Wazer, J., *Viscosity and Flow Measurement*, Wiley, New York, 1963.

Washington, C. and Davis, S., The production of parenteral feeding emulsions by microfluidizer. *Int. J. Pharm.*, 44 (1988) 169–176.